Journal of Computer-Aided Molecular Design (2006) 20: 109–130
DOI 10.1007/s10822-006-9040-8

Development of small molecules designed to modulate protein–protein interactions

Ye Che[a,*], Bernard R. Brooks[a] & Garland R. Marshall[b]
[a]*Laboratory of Computational Biology, National Heart, Lung and Blood Institute, National Institutes of Health, Bethesda, MD, 20892, USA;* [b]*Center for Computational Biology and Department of Biochemistry and Molecular Biophysics, Washington University, St Louis, MO, 63110, USA*

Received 31 October 2005; accepted 13 February 2006

Key words: conformational analysis, drug design, peptidomimetics, protein–protein interaction, protein-surface mimetics, privileged scaffold, template design

Summary

Protein–protein interactions are ubiquitous, essential to almost all known biological processes, and offer attractive opportunities for therapeutic intervention. Developing small molecules that modulate protein–protein interactions is challenging, owing to the large size of protein-complex interface, the lack of well-defined binding pockets, etc. We describe a general approach based on the "privileged-structure hypothesis" [Che, Ph.D. Thesis, Washington University, 2003] – *that any organic templates capable of mimicking surfaces of protein-recognition motifs are potential privileged scaffolds as protein-complex antagonists* – to address the challenges inherent in the discovery of small-molecule inhibitors of protein–protein interactions.

Introduction

Processes in living cells are largely controlled by proteins, sometimes alone, but more often in concert with partners. Cytoskeletal architecture depends upon large protein assemblies. Signals transduction from receptors embedded in the plasma membrane to specific intracellular sites are relayed by highly precise protein–protein associations. Cell–cell recognition is mediated through specific surface receptors. The immune response relies in large part upon the recognition of proteins and peptides by antibodies. Many regulated processes require initiation or inhibition via specific protein–protein complex formation; cytokine signaling and gene regulation are examples. Transcription is orchestrated by a plethora of transcription factors, activators, and suppressors, whose assembly is poorly understood, but clearly essential. Proteins often form a large complex network, in which they regulate and support each others, through protein–protein interactions. Given the ubiquitous nature of protein interactions and the knowledge that inappropriate protein–protein recognition can lead to disease, protein interactions offer attractive opportunities for therapeutic intervention based on selective inhibition of interactions between proteins. For example, aberrant protein–protein interactions associated with human diseases offer the possibilities as therapeutic targets for treatments, and specific protein–protein interactions in virus or bacteria not found in human hold the potential for treatment of infectious diseases ([1], for recent reviews on the development of small-molecule

*To whom correspondence should be addressed. Fax: +1-301-402-3404; E-mail: chey@nhlbi.nih.gov
This paper is adapted from a presentation at the 230th National Meeting of the American Chemical Society, Washington DC, August 28 – September 1, 2005, Abstract COMP-136.

inhibitors of protein–protein interactions see Refs [2–9]).

The design of small molecules to bind the active sites of enzyme has been remarkably successful. Enzymes, the catalysts of biological systems, accelerate reactions through selectively stabilizing the transition state relative to substrates. Thus, it is the transition state, instead of either substrates or products, that fits enzymes as a key fits a lock. The transition state is the least occupied species along the reaction pathway; by definition it is the one with the highest free energy. Linus Pauling [10] in 1948 proposed that stable compounds resembling the transition state of a catalyzed reaction should be very effective inhibitors of enzymes, so called transition-state analogs. The "transition-state analog" paradigm has been a guiding principle behind drug discovery targeting enzymes.

"Hot spots" of protein–protein interactions

In contrast, the development of small-molecule inhibitors of protein–protein interactions is widely considered to be difficult as no similar underlying theory provides a rational basis for design. Protein–protein interaction typically occurs over a relatively large surface area, on average approximately 800 ± 200 Å [2] of protein surface is buried on each side of the interface [11], vastly exceeding the potential binding area of a low-molecular-weight compound. In addition, the binding surfaces between two proteins tend to be relatively flat, and may lack crevices and pockets that provide snug binding sites for small molecules. Attempting to modulate such protein–protein interactions with cell-permeable small synthetic compounds appeared unfeasible to many at first glance. It is not necessary, in general, for a small molecule to cover the entire protein–protein interface, however, because the subset of the interface that contributes to high-affinity binding (the "hot spot" [12]) is often much smaller. Such hot spots of binding free energy may be a common feature of protein complexes. Hot-spot residues tend to be clustered together at the center of a protein-complex interface and are surrounded by energetically less important residues that probably serve to occlude bulk solvent [13]. Several studies have reported phage-display selection of small peptides that bind to protein hormones or receptors [14, 15]. Strikingly, these randomly selected peptides usually bind at the protein hot spot, even though they were not necessarily selected for protein–protein inhibition. These results suggest that hot spots at a protein-complex interface appear to be preferred owing to their intrinsic conformational and physiochemical properties, and they are particularly adept at binding to proteins, peptides and hopefully, small drug-like molecules. Further, a survey of experimental data on a large number of the strongest-binding protein-ligand [16] and protein–protein [17] interactions indicates that the free energy of binding increases with the number of non-hydrogen atoms with an initial slope of about 1.5 kcal/mol per atom. For ligands containing more than 15 non-hydrogen atoms, the free energy of binding increases very little as the molecular mass is increased. The fact that not all side chains are bound with equivalent high specificity should not be surprising. What is optimized by evolution is the kinetics of the system, as most systems are in dynamic equilibrium. If every side chain in a peptide was optimally bound with the same affinity as biotin (which is approximately the same size as an amino acid), then the cooperative combined affinities of the side chains of a small peptide would prevent dissociation from its receptor. In general, nature optimizes rates, not affinities.

Thus, protein–protein recognition may be concentrated in a few key anchor residues arranged in a particular three-dimensional arrangement. This has led to the concept of "protein-surface mimetics", compounds retaining those essential functionalities and the ability to display them in a characteristic three-dimensional pattern complimentary to the protein surface. Therefore, the first step towards protein-surface mimetics is usually to identify hot spot residues responsible for protein-complex recognition. Subsequently, the topography of these side chains is reproduced by similar non-peptidic functionalities on a rigid scaffold that positions the crucial recognition elements correctly.

Protein-recognition motifs

Numerous examples of the three-dimensional structures of proteins complexed with their biological partners have been determined by both X-ray crystallographic as well as modern NMR

spectroscopy. These provide a basis to determine the range of recognition motifs that are commonly used in biological systems. Major protein-recognition motifs (Table 1) are exemplified as below:

(I) Helix (α and 3_{10}) recognition is the most common in protein–protein and DNA/RNA-protein [18–20] interactions. For instance, actin is a "hub" for protein–protein interactions and participates in more protein interactions than any other known proteins. Complex structures of actin with its binding partners have revealed that the vast majority of actin-binding proteins share a common helical motif, providing a mechanism whereby actin-binding proteins compete for a common binding site [21]. On the other hand, when a helical structure serves as a recognition motif for numerous homologous protein complexes, such as those seen in two-component systems in bacteria, sequence variation along one face of the helix is often used to accomplish binding specificity.

(II) Alternatively, more than 1500 crystal and solution structures of proteases with their corresponding peptide inhibitors [22] show that local regions of the peptide bound to the active sites adopt an extended strand conformation, in which side chains are readily accessible and the amide bonds of the peptide backbone play significant roles in recognition. This is also true of MHC binding of antigenic peptides, especially the N- and C-termini of the antigenic peptides. β-sheet formation between proteins occurs widely in normal biological functions as exemplified by the dimerization interface of human immunodeficiency virus (HIV) protease [23], the binding of the Ras oncoproteins to their kinase receptors [24], the formation of cell–cell junctions through the interactions between PDZ or PTB domains with peptide segments from other proteins [25], etc. β-sheet formation is also critical in protein aggregation [26] which occurs in a variety of diseases and is a common feature of many neurodegenerative diseases, including Alzheimer's disease, Creutzfeldt-Jakob disease, and Huntington's disease.

(III) Protein domains that recognize proline-rich motifs are frequently involved in the regulation of cellular events such as signal transduction, cell cycle, protein trafficking, targeted proteolysis, gene expression, etc. [27]. These proline-rich motifs generally adopt an extend conformation known as the left-handed polyproline II (PPII) helix. There are at least six distinct families of proline-rich binding domains: the Src-homology 3 (SH3) domains [28], the WW domains [29], the EVH1 domains [30], the GYF domains [31], the UEV domains [32], and the single-domain profilin proteins [33]. The mechanism by which the immune system differentiates self from foreign is based on molecular recognition of short peptides (7–11 residues for class I and 13–17 residues for class II), proteolytically derived from their parent proteins, that are sandwiched between two receptors: the major histocompatibility complex (MHC) molecule on the surface of antigen presentation cells, and the T-cell receptor. There are two classes of MHC molecules with complementary T-cells: class I molecules interact with T-cells bearing CD8 proteins, while class II molecules are recognized by CD4-positive cells. MHC class I molecules usually recognize peptides in an extended strand conformation [34]; while MHC class II molecules always bind peptides in a PPII-like structure [35].

(VI) Turns, defined as sites where the peptide chain reverses its overall direction, are ideal recognition sites in proteins because they present side chains in a solvent-accessible arrangement around a compact folding of the peptide backbone [36].

Table 1. Ideal parameters for regular repetitive polypeptide conformations.

	Backbone torsional angles		Residues per turn	Translation per residue (Å)
	Φ (deg)	Ψ (deg)		
α-Helix	−57	−47	3.6	1.5
3_{10}-Helix	−49	−26	3.0	2.0
Antiparallel β-sheet	−139	+135	2.0	3.4
Parallel β-sheet	−119	+113	2.0	3.2
Polyproline I	−83	+158	3.3	1.9
Polyproline II	−78	+149	3.0	3.1

Examples of turns as recognition motifs can be readily found in numerous antibody complexes of peptide or protein antigens [37–39]. Peptide recognition by G-protein coupled receptors (GPCRs) is the primary means of intercellular communication in many diverse biological systems. In the absence of adequate GPCR samples to allow direct characterization of the complex, indirect approaches that probe the structure of the complexes can be based on structure-activity studies. The bound conformation of peptide ligands for over 100 GPCRs has been probed using this indirect approach. Consistently, peptide-activated GPCRs recognize ligand with turn structure [40].

Privileged structures

The implication is that the design of protein-surface mimetics may be based on certain protein-recognition motifs. The feasibility of using small drug-like molecules as surface mimetics of protein-recognition motifs has been demonstrated by isolated natural products as well as screening of synthetic compounds. Retrospective analysis of chemical structures has led to identify certain molecular scaffolds that are more frequently associated with higher biological activity than other structures. Thus, the concept of "privileged structures" has emerged [41]. The essence of privileged structures is that molecules based on a common chemical scaffold can bind to multiple, unrelated classes of receptors with high affinity. Examples of privileged structures include, for instance, the benzodiazepine scaffolds (Figure 1) that have been utilized by Evans et al. [41] to mimic numerous reverse-turn motifs [42]. The benzodiazepine scaffold is the core element of the natural product aspercilin. The benzodiazepine derivatives are also found as CCK-A antagonists, benzodiazepine antagonists, neurokinin-1 antagonists, as enzyme inhibitors such as κ-secretase inhibitors and farnesyl transferase inhibitors, and as ion channel ligands such as the delayed rectifier K^+ current modulators [43]. The benzodiazepine analogs continue to generate leads against multiple protein receptors [44–48]

Herein, we summarize and prescribe methods for the design of small-molecule inhibitors of protein–protein interactions based on the "privileged-structure hypothesis" – *that any organic templates capable of mimicking surfaces of protein-recognition motifs are potential privileged scaffolds as protein-*

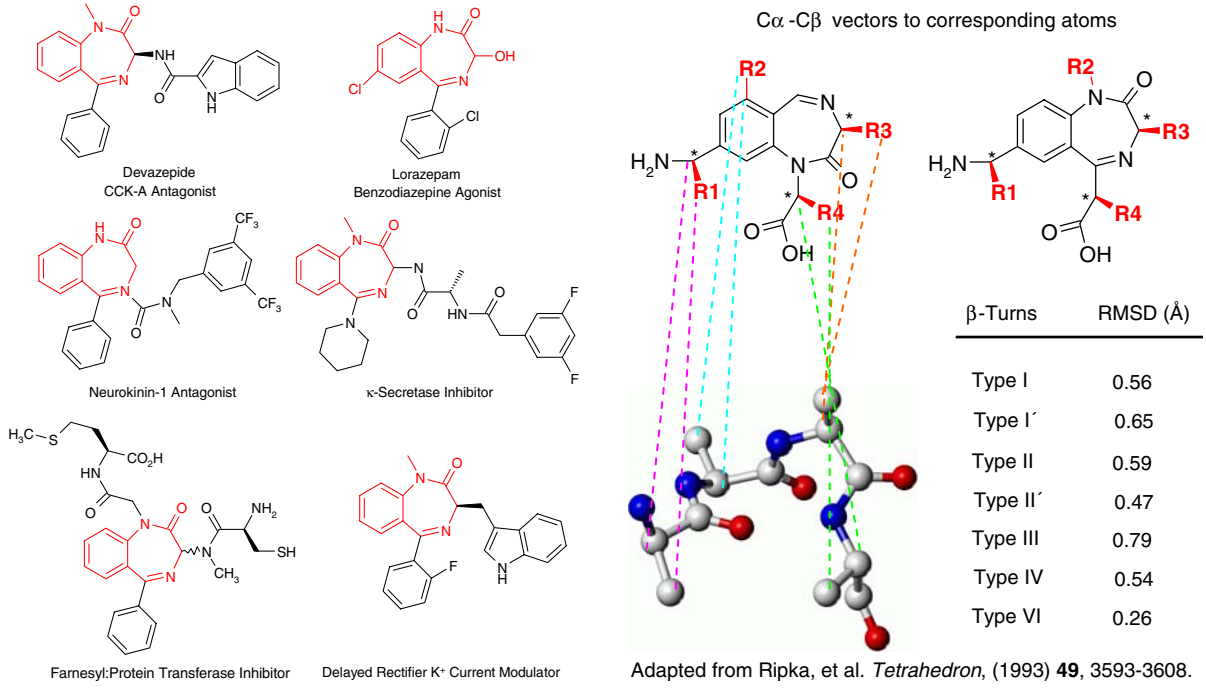

Figure 1. The benzodiazepine scaffolds suggested as privileged in deriving drugs that interact with different GPCRs (left); and the geometrical overlap of C_α–C_β vectors of peptide reverse-turn with substituents of benzodiazepine scaffolds (right).

complex antagonists. Protein-recognition motifs comprise repetitive structures such as helix, strand, and PPII, and non-repetitive structures such as turns. Here, we highlight recent advances in the mimicry of helical surfaces and reverse-turn motifs as illustrative examples to address the challenge and therapeutic potential of modulating macromolecular interactions in biological systems.

Mimicry of protein-recognition motifs

Mimics of helical surface and function

Helical structures represent one of the most common structural motifs and recognition sites in proteins. Helices are found in proteins predominately as α-helices (3.6 residues per turn), but occasionally as 3_{10}-helices (3 residues per turn). α-Helical motifs are dominant in many recognition processes. For example, sequence-specific DNA-binding proteins often employ α-helical motifs for DNA recognition; the fusion of viral membranes with target-cell membranes is an essential step in viral pathogenesis, and viral fusion proteins often form a stable six-helix bundle to bring both the viral and target cell membranes into proximity; α-Helices also play crucial roles in many signaling proteins mediating protein–protein recognition, such as G-proteins, BH3 domains, and calmodulins. 3_{10}-Helices are also involved in a number of protein recognition events. For instance, the SH3 domain, which normally recognizes proline-rich sequences, has the potential to bind RxxK motifs with a 3_{10}-helix conformation [49]; the 3_{10}-helix regions in cyclin-dependent kinase inhibitors are indispensable for inhibition and growth suppression [50]. In isolated helices, transition between the α- and 3_{10}-forms is facile with an estimated energy barrier in the region of 3–4 kcal/mol [51]. Helix geometry of the peptide backbone allows a single NH group to make two weaker bifurcated H-bonds in the transition state between the α- and 3_{10}-helix. The lowness of this barrier suggests that small peptide helices can easily be induced to bind in either helical conformation by interaction with their receptor. One goal is to design helix mimetics that can distinguish between the two helical surfaces by fixing the position and relative orientation of side chains.

Helix-stabilizing approaches

Short synthetic peptides corresponding to biologically active helical motifs within proteins typically have little structure when taken out of context and placed in water; without additional constraints, the modest advantage of intrachain H-bonds and side chain – side chain interactions in helix is insufficient to overcome the penalty of conformational restriction. It is estimated that elimination of a single rotational degree of freedom of a peptide by preorganization stabilizes the receptor-bound conformation should enhance affinity by approximately 1.2–1.6 kcal/mol assuming complete loss of rotational freedom [52]. Thus, preorganization of a 10-residue helical segment with multiple (18–20) rotational degrees of freedom in the peptide backbone, for example, fixed into its bound conformation should enhance the binding affinity by several orders of magnitude. Accordingly, numerous strategies have been developed to stabilize helical conformation in a peptide

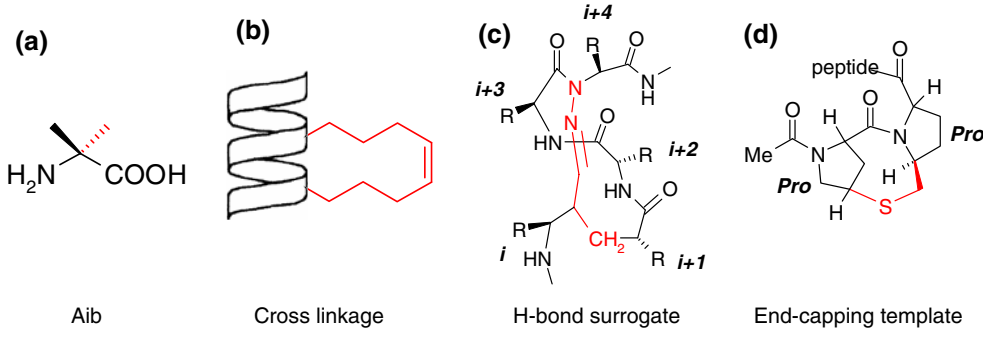

Figure 2. Helix-stabilization methods. (a) α,α-disubstituted unnatural amino acids; (b) cross-linked interfacial peptides; (c) intrachain H-bond mimetics; and (d) end-capping templates.

(Figure 2). Marshall and Bosshard [53] predicted by computation in 1972 that α,α-dialkyl amino acids, such as α-methylalanine or aminoisobutyric acid (Aib), would severely restrict the Φ and Ψ torsion angles of that residue to those associated with right- or left-handed helices (both α- and 3_{10}-helices), due to steric interactions involving the *gem*-methyl groups linked to the α-carbon. Subsequent experimental validation of that prediction is abundant, from the Marshall lab [54] as well as others [55–57]. An example where α,α-dialkyl amino acids were used to induce a helix of the peptide in water that enhanced binding involves the p53/hdm2 helix recognition ($IC_{50} = 5$ nM versus 8673 nM) [58]. Alternatively, the helical structure could be stabilized through the incorporation of covalent or noncovalent linkages between the side chains of two residues separated in sequence, but spatially close in a helix, such as residues *i* and $i+4$ of an α-helix or residues *i* and $i+3$ of a 3_{10}-helix, respectively. Examples of chemical linkages that enhance helical propensity are salt bridges [59] hydrophobic interactions [60, 61] aromatic-charge [62] or aromatic-sulfur [63] interactions, disulfide bonds [64, 65], lactam bridges [66–72], hydrocarbon staplings [73–75], diaminoalkanes [76] acetylenes [77], and metal ligation between natural [78–82] and unnatural amino acids [83, 84]. These cross-linked peptides have been demonstrated to yield a marked enhancement of peptide helicity, stability, and *in vitro* and *in vivo* biological activity. For example, the interaction between the pro-apoptotic protein BID and the anti-apoptotic protein Bcl-x_L was targeted by a hydrocarbon-stapled helix [75]. This constrained helical segment, derived from the helical BH3 domain of BID, was found to be protease resistant, cell-permeable, and bound to Bcl-x_L with a six-fold higher affinity than the unconstrained helix ($K_d = 38.8$ nM versus 269 nM). Cellular uptake was observed and apoptosis was activated within cells upon treatment with the constrained helix. In addition, the constrained helix effectively inhibited the growth of human leukemia xenografts *in vivo*. Helical peptides are stabilized by extensive, but weak intrachain H-bonds. This has led to the design of covalent mimics of the intrachain H-bonds to reinforce helical conformation [85, 86]. Such artificial helical peptides are attractive scaffolds for molecular recognition, since the main chain H-bond surrogate either blocks solvent-exposed recognition surface or removes important side chain functionalities. For example, one peptide analog of a human papillomavirus peptide segment was conformationally restricted to an α-helix structure using the hydrazone link (N–H = CH–CH2CH2) approach and was shown to have a very strong reaction with sera from women having invasive cervical carcinoma [87]. Though the main body of the helix is stabilized by intrachain H-bonds, there will necessary be free NH groups at the N-terminus and CO groups at the C-terminus of the helix, which cannot participate in such H-bonding. Accordingly, preorganized helix-nucleating templates [88–95] in which the orientation of the first four NH groups or the last four CO groups is fixed in a rigid structure, have been designed to initiate helix formation and prevent fraying of the ends. For example, a series of preorganized templates, designed to take advantage of the known N-capping properties of Pro, was shown to induce helicity even in short peptides.

Helical foldamers

A hand of unnatural oligomers (Figure 3 and Table 2) with a strong tendency to adopt helical structures has also been described to target protein-complex interfaces. Many of these are structural variants of polypeptides but are essentially invulnerable to proteases. One such family of

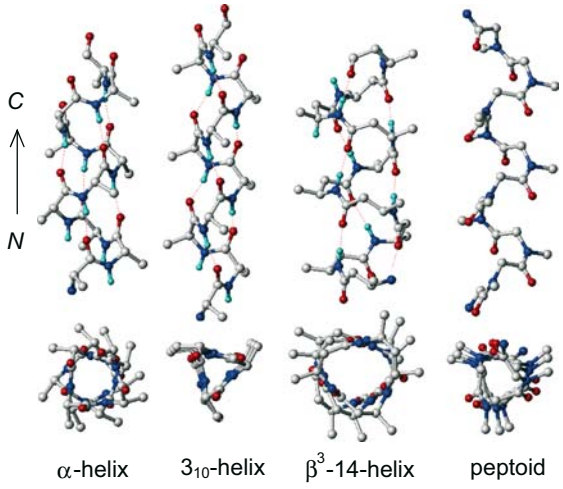

Figure 3. Schematic comparison of α-helix, 3_{10}-helix, β^3-14-helix, and peptoid helix, formed by α-amino acids, β^3-amino acids, and N-substituted glycines, respectively.

Table 2. Ideal parameters for α-helix, 3_{10}-helix, β^3-14-helix, and peptoid helix.

	Backbone torsion angles				Residues per turn	Pitch (Å)	H-bond	Macrodipole
	ω (deg)	ϕ (deg)	θ (deg)	ψ (deg)				
α-Helix	*trans*-	−57	–	−47	3.6	5.4	1 ← 5	N → C
3_{10}-Helix	*trans*-	−49	–	−26	3.0	6.0	1 ← 4	N → C
β^3–14-Helix	*trans*-	−134	60	−140	3.0	4.7	1 → 3	C → N
Peptoid	*cis*-	−70	–	165	3.0	6.0	None	C → N

oligomers is the poly-N-substituted glycines or "peptoids" [96] on which the side chains are appended to the amide nitrogens rather than the α-carbons. Despite the achirality of the N-substituted glycine backbone and its absence of H-bond donors, peptoids containing α-chiral, sterically bulky side chains are able to adopt stable, chiral helices with *cis*-amide bonds. The periodicity of this peptoid helix is three residues per turn, with a pitch of 6 Å [97] which is very similar to that of the 3_{10}-helix. The other family of oligomers is the β-peptides [98, 99], which differ from α-peptides by one additional backbone carbon atom. β-peptides composed of β^3-L-amino acids are able to form left-handed 14-helices characterized by a periodicity of three residues per turn with a pitch of 4.7 Å, and H-bonds between the backbone amide proton of residue i and the carbonyl oxygen of residue $i+2$. The ability to form stable helices makes peptoids and β-peptides good candidates for mimicry of bioactive peptides that rely on helical structure for proper function. For example, the Appella group has developed peptoids that inhibit the p53-hdm2 interaction [100], and the Schepartz group has designed adaptable β-peptide scaffolds with enhanced 14-helix structure by neutralization of the helix macrodipole [101] and developed helical β-peptide inhibitors of the p53-hdm2 interaction [102] and the gp41-mediated HIV-1 fusion [103].

Helical surface mimetics

Since the critical interactions for α-helix recognition often involve the side chains of residues i, $i+3$ and/or $i+4$, and $i+7$, along one face of the α-helix, it is possible to design appropriate scaffolds with limited conformations that can orient attached functional groups to correctly resemble the α-helical surface and function generated by these key residues (Figure 4). There are 3.6 residues per turn of the α-helix, with a rise of 1.5 Å per residue. The characteristic axial rise between these key residues is 4.5 Å or 6.0 Å, respectively. Looking down the helical axis, residues are projected at −60° and 40° for $i \rightarrow i+3$ and $i \rightarrow i+4$ interactions, respectively. Hamilton and his co-workers described a terphenyl scaffold that can reasonably imitate the α-helical surface in which the 3,2′,2″-substituents on the phenyl rings present functionalities in a spatial orientation that mimics the i,

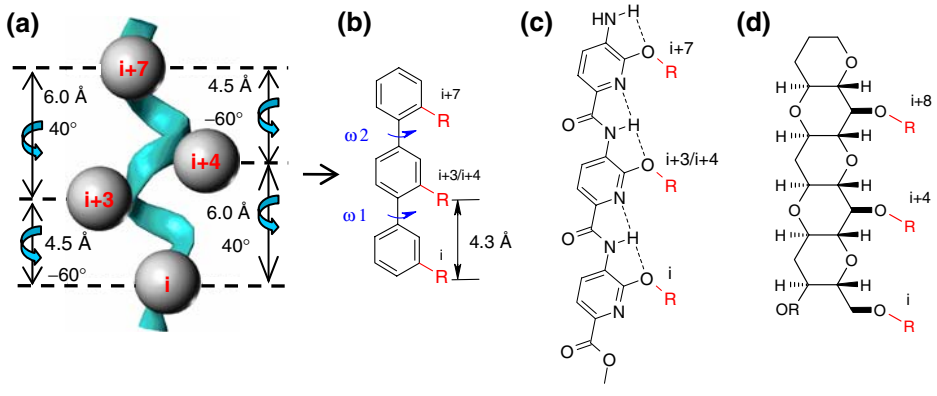

Figure 4. Idealized α-helix geometry (a) with 4.5 or 6 Å rise between residues i, $i+3$, $i+4$, and $i+7$ of an α-helix, all located on same face of the helix. Prototypes of α-helical surface mimetics: (b) the terphenyl scaffold; (c) the trispyridylamide scaffold; and (d) the *trans*-fused polycyclic ether scaffold.

$i+3$ or $i+4$, and $i+7$ residues on an α-helix [104–108]. Comparing the ideal α-helical structure and the terphenyl scaffold, when the terphenyl is in a staggered conformation with $\omega_1 = -60°$ and $\omega_2 = 40°$, the three substituents project from the terphenyl core with similar angular relationships and 5–30% shorter distances in the characteristic rise corresponding to $i \rightarrow i+3$ or $i \rightarrow i+4$ interactions in a native helix, respectively; when the terphenyl scaffold is in another staggered conformation with $\omega_1 = 40°$ and $\omega_2 = -60°$, the three substituents correspond to the i, $i+4$, and $i+7$ positions. Proof of concept came from successfully disrupting the interaction between calmodulin and an α-helical domain of smooth muscle light-chain kinase [104], inhibiting the self-assembly of HIV gp41 and reducing levels of viral entry into host cells [105], preventing the interaction between the pro-apoptotic protein Bak and the anti-apoptotic protein Bcl-x_L [106, 107] and blocking the complex formation of the tumor-suppressor protein p53 with the oncoprotein hdm2 [108]. Based on theoretical arguments, Jacoby [109] also suggested that 2,6,3′,5′-substituted biphenyls as better than allenes, alkylidene cycloalkanes and spiranes as α-helix mimetics of residues i, $i+1$, $i+3$, $i+4$. The low solubility of the terphenyl scaffold in polar solvents has led the Hamilton group to the development of another class of helical surface scaffold, the trispyridylamide [110]. The template adopts a preferred conformation in which all three functional groups are projected on the same face of the scaffold. This preorganization is accomplished through a stabilizing bifurcated H-bonding network as well as through the minimization of alternative conformations. The polyamide backbone was shown to be quite planar, based on MM2 energy minimization, with the characteristic axial rise of 5.7 Å, close to that of the $i \rightarrow i+4$ interaction in a native helix. The alkoxy side chains, however, are rotated approximately 45° out of the plane of the carboxamide backbone, presumably to optimize the position of the lone-pair electrons on the oxygen atom of the ether functionalities for H-bonding. This may explain why those analogs had maximal binding affinities only in the low μM for Bcl-x_L, compared to a K_d value of 114 nM for a terphenyl derivative and 300 nM for the 16-residue BH3 domain peptide from Bak. More recently, the *trans*-fused 6/6/6/6/6 pentacyclic ether skeleton, the core template of marine toxins, was also suggested to imitate residues i, $i+4$, and $i+8$ of an α-helix.

Conformational restriction

Compared to other templates containing a chiral axis, the terphenyl is a typical drug-like scaffold. In a retrospective analysis of privileged structures of pharmacologically active compounds, biaryls were found to be present in 7.4% of reference drug molecules. Therefore, the terphenyl and its derivatives represent an attractive way to interfere with helix recognition and contribute to enlarge the scope of peptidomimetics. However, the terphenyl scaffold is not rigid; for example, it could adopt both right- and left-handed twists. There are sixteen energetically almost equal conformers, and among them only two can mimic the desired α-helical twist (Figure 5). And, it was estimated, based on the Boltzmann-weighted distribution from the DFT (B3LYP/6–31G*) calculation, that only about 5.9%, slightly less than one sixteenth (6.25%), of the whole ensemble exhibits the characteristic twist of residues (i, $i+3$, $i+7$) or (i, $i+4$, $i+7$) of an α-helix (Table 3, Figure 6). These suggested that the original terphenyl scaffold is limited in terms of α-helical mimicry due to the conformational heterogeneity. Therefore, various other organic scaffolds had been evaluated [1] as helix mimetics to determine how well they can orient side chains in positions corresponding to side chains of α- or 3_{10}-helices. One aspect of the selection procedure is the rigidity introduced by the scaffold. As an example of one alternative scaffold, the terpyridyl scaffold (Figure 5) is much more rigid and limits side chain orientation to a greater extent than does the terphenyl scaffold [1]. The twist between adjacent aromatic rings is balanced by two competing factors of the same order of magnitude, namely the symmetry interaction between the π orbitals of the aromatic rings (the electron delocalization effect) and the steric repulsion between overlapping *ortho* hydrogen atoms and substituents. The former prefers a coplanar arrangement, while the latter tends to force the molecule to be nonplanar. Balance of these two factors results in a twisted structure. It is well-known that the twist angle (ω)is about 45° for the biphenyl without any substituents. For steric reasons, substitution of the *ortho* hydrogen by a larger atom or group leads to a double minimum potential, with the twist angle of the syndiagonal

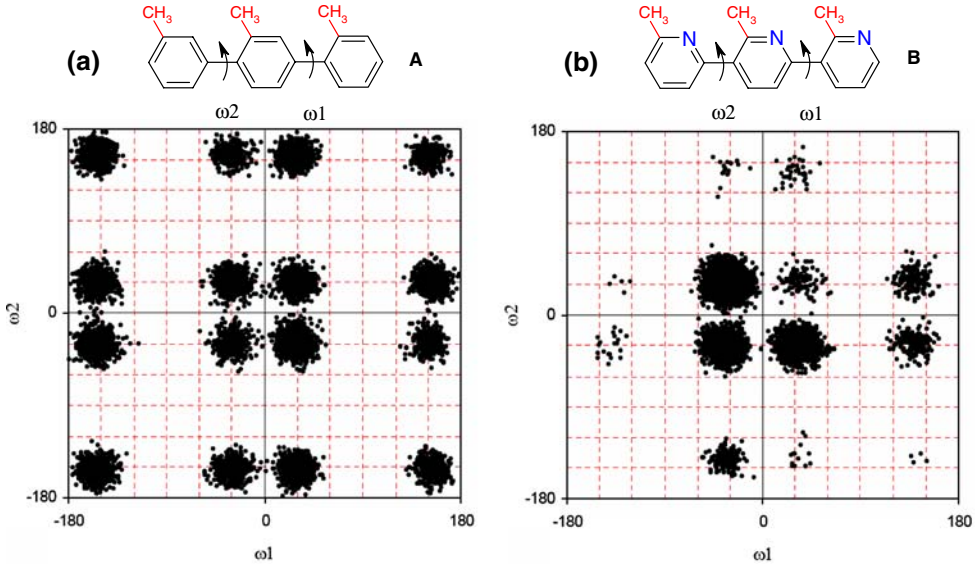

Figure 5. (a) The 3,2′,2″-*tris*-substituted-terphenyl scaffold and (b) the 6,6′,2″-*tris*-substituted-terpyridyl scaffold with three methyl groups representing substituents, and their canonical ensemble from mixed Monte Carlo – stochastic dynamic (MC/SD) simulations done with the OPLS-AA force field and the GB/SA water model. (This figure is for the illustrative purpose only, because the generic force-field parameter set used was not optimized for this series of compounds.) [1].

Table 3. The helical mimicry population (p) of triaryl scaffolds and the structural and energetic features of their corresponding biaryl model compounds. All were estimated at the B3LYP/6-31G* level of theory.

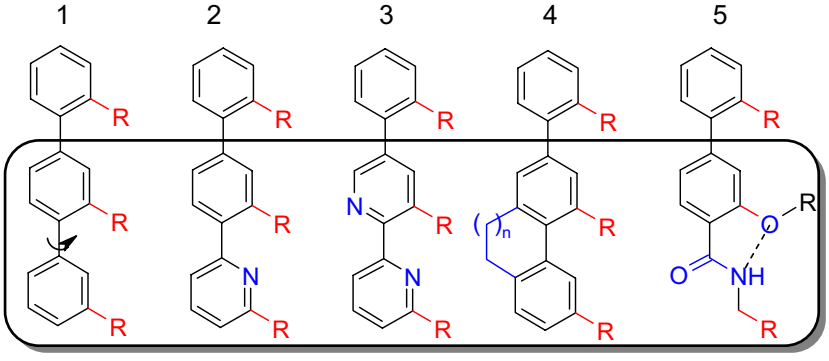

	Biaryl model compounds (**1′**–**5′**)					Triaryl scaffolds (**1**–**5**)
	ω (*syn*)	[a]ΔE^{α}	[b]ΔE^{0}	[b]ΔE^{90}		p ($-90° < \omega_1 < 0°$, $0° < \omega_2 < 90°$) or p ($0° < \omega_1 < 90°$, $-90° < \omega_2 < 0°$)
1′	57.1°	0.01	7.21	0.55	**1**	5.9%
2′	43.7°	−0.74	2.71	2.15	**2**	9.9%
3′	17.4°	−5.25	0.03	4.91	**3**	11.9%
4′	32.1°	–[c]	4.68	17.68	**4**	12.1%
5′	2.1°	−5.24	0.00	5.94	**5**	10.1%

[a]*Syn-anti*-twist energy differences: $\Delta E^{\alpha} = E$ (*syn*)$-E$ (*anti*).
[b]Rotational barriers: $\Delta E^{0} = E$ ($\omega = 0°$)$-E$ (*syn*), $\Delta E^{90} = E$ ($\omega = 90°$)$-E$ (*syn*).
[c]Single minimum potential profile without an antidiagonal form.

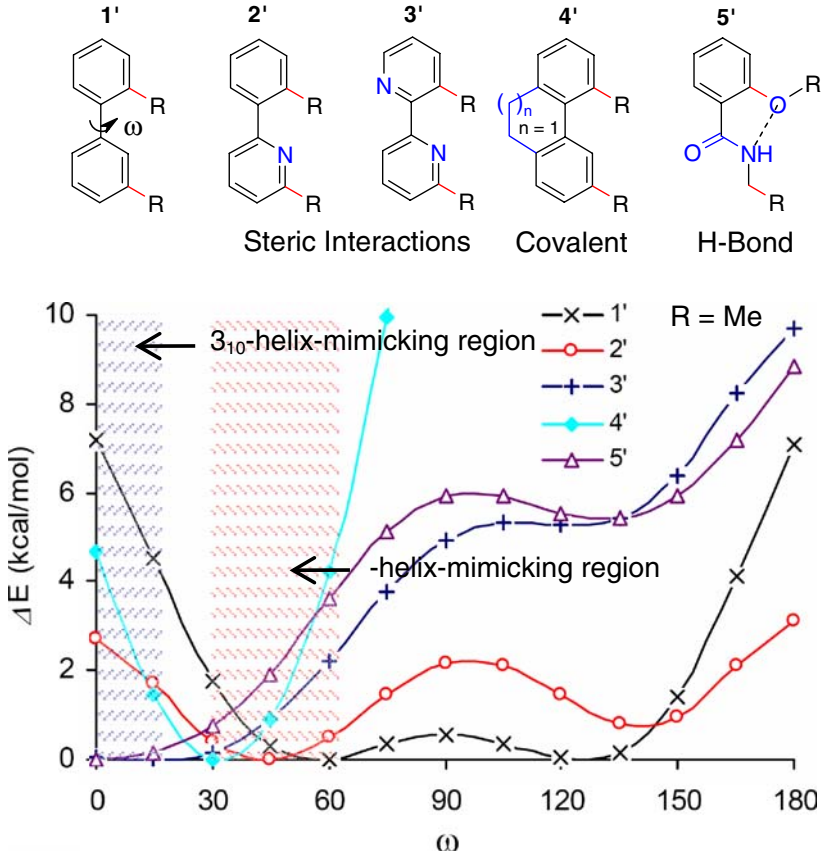

Figure 6. The relative energy as a function of ω angle for the biaryl model compounds, estimated at the B3LYP/6-31G* level of theory.

form ($0° \le \omega \le 90°$) being larger than the biphenyl value of 45°, and ω of the antidiagonal form ($90° \le \omega \le 180°$) being smaller than 135°, with the antidiagonal structure being lower in energy. On the other hand, for the same reason, replacement of the phenyl ring with a pyridyl ring leads to a less twist structure ($\omega \le 45°$ or $\omega \ge 135°$) due to a weaker repulsion between the nitrogen lone pair and the hydrogen atom from the adjacent ring, with the syndiagonal form being favored by 0.74 kcal/mol determined at the B3LYP/6–31G* level of theory (Table 3). The percentage of the time that the (i, $i+3$, $i+7$) or (i, $i+4$, $i+7$) orientation of side chains would be populated in the pyridyl–biphenyl scaffold (2) with a single pyridyl ring has risen to nearly 10% of the time. Such conformational enrichment should be doubled in the terphenyl scaffold as can be appreciated by directly comparing the distribution in Figure 4. The total percentage of α-helical content would be 38.4% for the terpyridyl scaffold and only 11.8% for the terphenyl scaffold. Furthermore, the rotational barrier at 0° [$\Delta E^0 = E(\omega = 0°) - E(syn$ equilibrium)] has been reduced from about 7.2 kcal/mol in compound 1′ to about 2.7 kcal/mol in 2′, and the rotational barrier at 90([$\Delta E^{90} = E(\omega = 90°) - E(syn$ equilibrium)] has been increased from about 0.6 kcal/mol in 1′ to about 2.2 kcal/mol in 2′. These results suggest that pyridyl-based scaffolds are more flexible in the α-helix mimicking regions and can more easily interconvert between syndiagonal minima. Such flexibility may be helpful to allow some optimization of binding interactions due to induced fit. Our tentative conclusion is that the terpyridyl scaffold should be superior as a helical surface mimetics to be reflected in enhanced binding affinity and lower loss of entropy on binding. The terpyridyl scaffold augments the propensity in α-helix mimicry through unbalanced steric interactions. Synthetic accessibility of

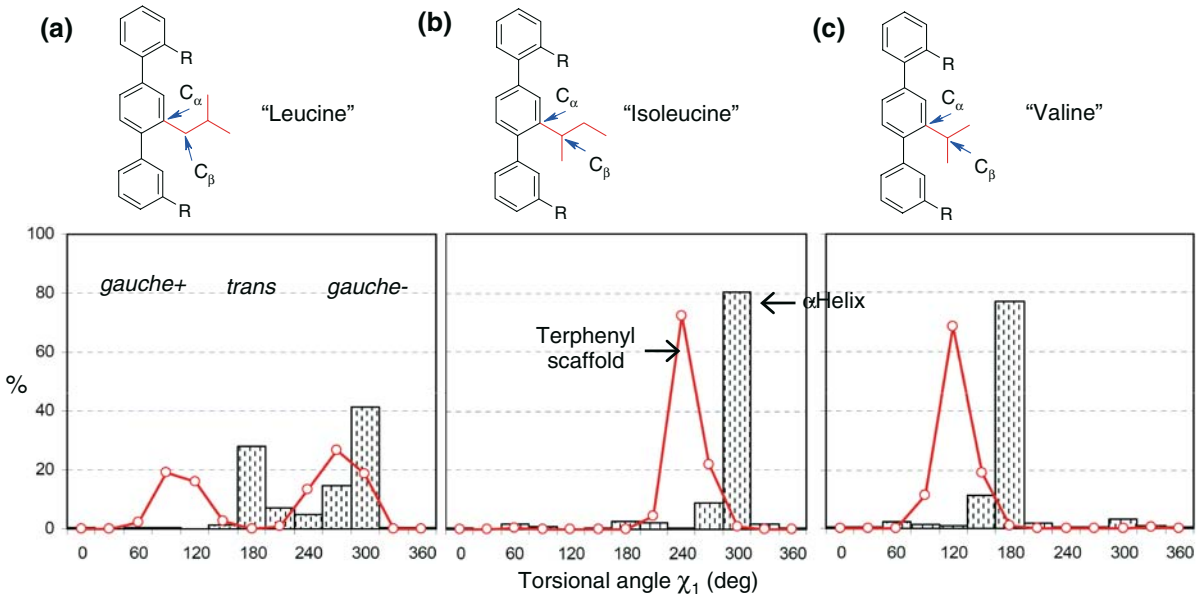

Figure 7. Histogram of the side chain rotamers (C_α–C_β torsion angle χ_1) observed for Leu, Ile, and Val residues in the helical conformation from high resolution protein crystal structures, and comparison with those distributions in the terphenyl derivatives as the terphenyl axis aligned with the helix axis. The rotamer distribution of terphenyl derivatives was estimated using the MC/SD simulations done with the MM2 force field and the GB/SA water model (R = Me).

substituted terpyridyl derivatives has recently been demonstrated by Hamilton and his co-workers using sequential Bohlmann–Rahtz heteroannulation reactions [111]. Conformational restriction can also be achieved through the use of covalent linkages (scaffold 4) and H-bonds (scaffold 5) along one face of the scaffolds.

Side chain rotamers

An equally important area for the design of surface mimetics is that of the side chain orientation beyond the C_α–C_β bonds. Generally, rotations about the bonds of the side chains (χ_1, χ_2, etc.) are close to one of the three conformations (*trans*, *gauche*$^+$ and *gauche*$^-$) in which the attached atoms are staggered, with the conformation that gives the greatest separation of the bulkiest groups being favored. Those preferred side chain conformations are often referred as side chain rotamers. In helices, the side chains project outward into solution, although they are tilted toward the amino end of the helix, and need not interfere with the helical backbone. There are, however, varying restrictions on conformation of the side chains. In particular, the g^+ rotamer of angle χ_1 between the C_α and C_β is almost forbidden because any side chain would overlap atoms of the previous turn of the helix. Side chains with branched C_β atoms (Val, Ile, and Thr) are most restricted in their conformations. Our calculations indicated that the terphenyl scaffold also restricted side chain orientations (Figure 7), due to the steric repulsion with *ortho*-carbons on the same phenyl ring. Rotamer distributions of the terphenyl scaffold were similar to those of α-helices, but the profile of the χ_1 value for all side chain groups had a 60° shift compared to those of α-helices, as the terphenyl axis is aligned with the helix axis. Determination of the 3D structure of these small molecules bound with proteins and comparison with α-helix recognition motifs is an active area of research.

(i, i+3, i+7) or (i, i+4, i+7)-Selective α-Helix mimetics

The characteristic distances along the axis between the three substituents, for both the terphenyl and terpyridyl scaffolds, are all 4.3 Å which is approximately 5% shorter than that of the $i \rightarrow i+3$ geometry in a native α-helix and 30% shorter than that of the $i \rightarrow i+4$ geometry. Such arrangements cannot differentiate between the specific recognitions through residues i, $i+3$, $i+7$ with that of residues i, $i+4$, $i+7$. In addition, compounds based these scaffolds might bind to the receptor

in an alternative orientation, either the $N \rightarrow C$ direction or the $C \rightarrow N$ direction, if all three substituents are similar. We suggested that shift of one substituent along the axis (for example, through the use of naphthalene) increases one characteristic distance to about 6.5 Å, close to the $i \rightarrow i+4$ geometry [1]. Depending on the position of the naphthalene ring and the position of substitution sites, new templates can selectively mimic the orientation of side chains i, $i+3$, $i+7$ or i, $i+4$, $i+7$ of an α-helix. To use an amide bond as a linker between adjacent phenyl rings, instead of a phenyl–phenyl single bond, can result in a similar effect on the characteristic distances. Similarly, the incorporation of appropriate polycyclic rings, such as thieno[3,2-b]pyrrole, is also able to place a substituent in the $i \rightarrow i+4$ geometry. Alternatively, Jacoby [109] proposed that 2,6,3′,5′-substituted biphenyl analogs as α-helix mimetics superimposing the side chains of the residues i, $i+1$, $i+3$ and $i+4$. This opens the possibility to mimic all those critical residues along one face of an α-helix with terphenyl derivatives (Figure 8). The combination of many of the modifications just mentioned within a single framework might lead to an even better helix mimetics with improved conformational preference. Knowing that many protein–protein interactions of potential therapeutical relevance involve α-helix contacts, this diversity of helical scaffolds offers novel ways to interfere within such targets.

Mimics of turn surface and function

Most proteins have compact, globular shapes, requiring reversals in the direction of their polypeptide chains to accommodate packing. Many of these reversals are accomplished by a common structural element called the reverse turn. Receptor recognition, substrate specificity, and catalytic function generally reside in these loop regions that often connect residues of the α-helices and β-strands contributing to the structural stability of proteins. β-Turns, the most common type of reverse turn comprised of four residues, are often stabilized by an intramolecular H-bond between the CO group of residue i to the NH group of residue $i+3$. Turns are the most common type of non-repetitive structures and comprise nearly one-third of the residues of globular proteins. They invariably lie on the surface of proteins, and often necessarily participate in interactions between proteins and other molecules based on their location. Several types of "classic" β-turns are possible depending upon the Φ and Ψ backbone torsion angles of residues $i+1$ and $i+2$, shown in

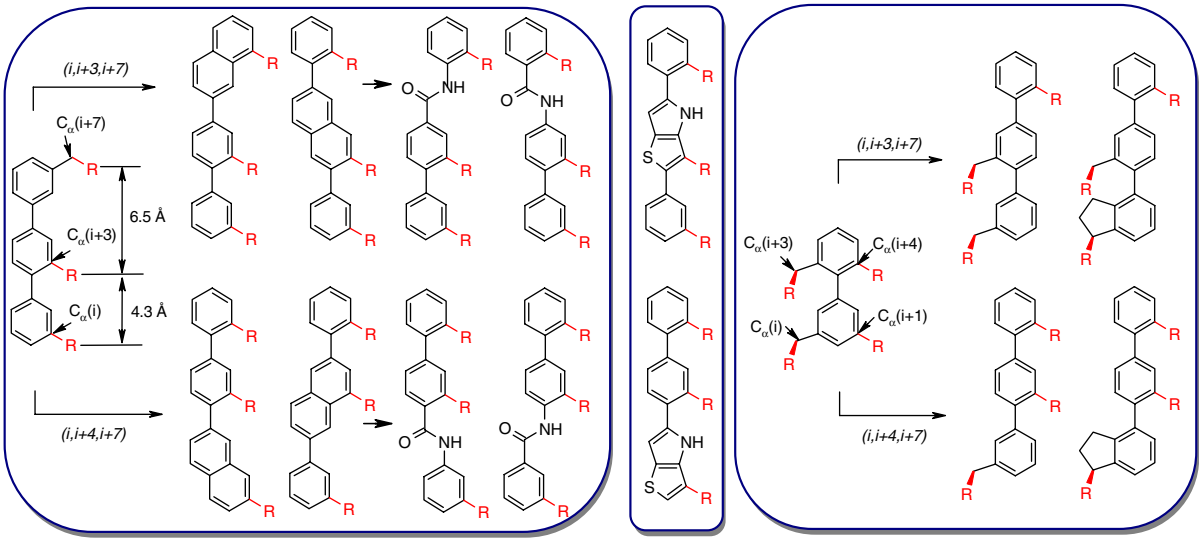

Figure 8. Helix mimetics designed to selectively mimic the orientation of side chains i, $i+3$, $i+7$ or side chains i, $i+4$, $i+7$, or all four residues along an α-helix: (left) shift of one substituent along the axis increases one characteristic distance to 6.5 Å, close to the $i \rightarrow i+4$ geometry; (middle) incorporation of appropriate polycyclic rings, such as thieno[3,2-b]pyrrole, have a similar effect; (right) Extension of a methyl (to become an ethyl) can expand the scaffold to mimic the orientation of both side chains i, $i+1$ in a single ring.

Table 4. Ideal backbone torsion angles for classic β-turns.

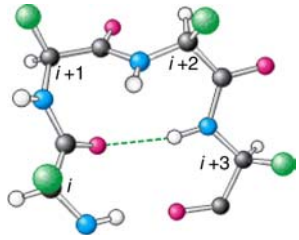

.

Class	Φ_{i+1} (deg)	Ψ_{i+1} (deg)	ω_{i+1} (deg)	Φ_{i+2} (deg)	Ψ_{i+2} (deg)
Type I	−60	−30	180	−90	0
Type I′	+60	+30	180	+90	0
Type II	−60	+120	180	+80	0
Type II′	+60	−120	180	−80	0
Type V	−80	+80	180	+80	−80
Type V′	+80	−80	180	−80	+80
Type VIa	−60	+120	0	−90	0
Type VIb	−120	+120	0	−90	0
Type VIII	−60	−30	180	−120	+120

Table 4. Type I β-turn occur most frequently, two to three times more frequently than type II. The mirror-images (of the backbone, but not the side chains) types I′ and II′ are rare, but type I′ is preferred as the connector in β-hairpins, presumably because it fits the twist of the β-sheet. Pro and Gly have a greater propensity than other naturally occurring amino acids to be found in β-turns. Pro predominates at position $i+1$, and Gly predominates at position $i+3$ of both type-I and type-II turns. One special type of β-turn is the type-VI turn defined by an amino acid, usually Pro, with a *cis*-amide bond located between residues $i+1$ and $i+2$. An example of the type-VI turn as a loci for molecular recognition can be found in the solution structure of an antibody-bound HIV-1_{IIIB} V3 peptide [112]. In addition, such a type-VI turn conformation in the HIV-1_{IIIB} V3 peptide was entirely consistent with antibody recognition deduced from structure-activity studies [113].

The design of mimetics that constrain a peptide to adopt a reverse turn is an important aspect of modulating protein–protein interactions. The dipeptide lactam [114], the bicyclic dipeptide BTD [115], and similar proline derivatives [116], spirolactam–bicyclic and tricyclic systems based on proline [117–120], substitution by N-amino proline [121] and dehydro amino acids [122–125] and metal complexes of linear peptides [126] are all examples which partially constrain the four backbone torsion angles of residues $i+1$ and $i+2$ and enhance reverse-turn propensity (Figure 9). Other efforts have focused on stabilizing type-VI turn with a *cis*-amide bond between residues $i+1$ and $i+2$ through using the 1,5-disubstituted tetrazole [127–130], 1,2,5-triazole [131], or 1,2,4-triazole [132] as

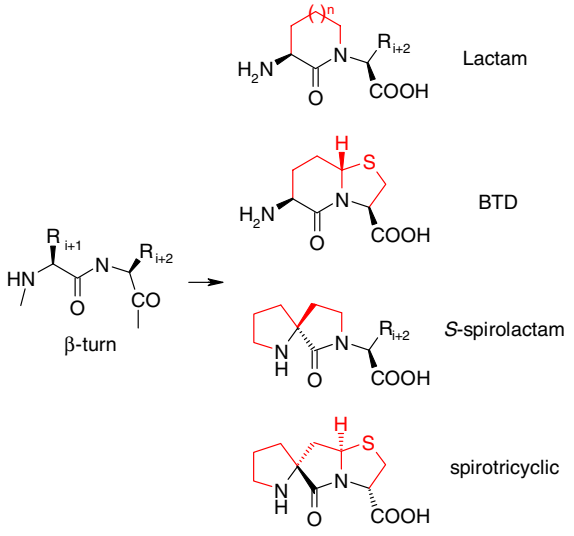

Figure 9. Representative compounds used to stabilize the reverse turn in a peptide chain.

cis-amide bond surrogates, incorporating vicinal disulfide bonds [133, 134], bicyclic dipeptide analogs [135–137], and certain sequences into cyclic peptides [138]. Alternatively, based on the unique role of Pro in *cis-trans* isomerization and its high frequency within type-VI turns, several methods have been employed to stabilize the *cis*-amide bond through chemically modifying Pro residues [139]: substituting sterically bulky groups at the δ-carbon of Pro; [140, 141] introducing oxaproline or thioproline (often denoted as pseudoproline), the oxazolidine or thiazolidine-derived Pro analogs [142]; and incorporating the amino acid analog azaproline [143–145] in which the α-carbon is replaced with a nitrogen atom (Figure 10). The incorporation of some of these *cis*-Pro analogs into proteins/peptides has led to enhanced binding or metabolic stability. For example, a thioproline-derived synthetic protein, PSC-RANTE, which was 50 times more potent than apo-RANTE, dramatically improves the protein ability to prevent entry of HIV into cells by binding to the receptor CCR5 [146].

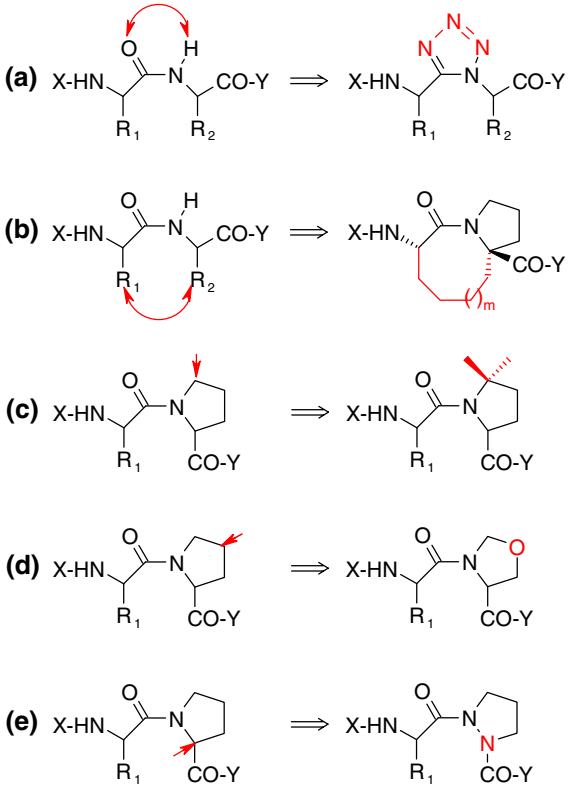

Figure 10. *cis*-Amide bond mimetics. (a) 1,5-disubstituted tetrazole, (b) bicyclic dipeptide, (c) 5-alkyl proline, (d) pseudoproline, and (e) azaproline.

Organic scaffolds have also been explored for β-turn recognition by appending desired substituents at selected positions. It was Hirschmann *et al.* [147, 148] who conducted the pioneering work and successfully demonstrated the use of β-D-glucose as a scaffold in the synthesis of somatostatin analogs, in which the whole peptide backbone was replaced by a saccharide, targeting the somatostatin receptors. Three residues, FWK, contain the necessary functional information, but it is the relative positioning of these side chains in space that determine the affinity for one or more of the somatostatin receptors. Substituents mimicking these amino-acid side chains were positioned on a β-D-glucose scaffold in a way that ensured that the distances between the pharmacophoric groups were similar to those of somatostatin. The Hirschmann group later demonstrated that compounds with modulated receptor subtype affinity are obtained by altering stereochemical centers in the scaffold. D-Glucose, L-glucose and L-mannose structural isomers were synthesized and displayed different subtype selectivity for somatostatin receptors [149]. Marshall and his co-workers [150] showed that metal complexes of chiral pentaazacrowns (MAC), derived by reduction of cyclic pentapeptides, fixed side chains in orientations comparable to those of ideal β-turns. The minor changes in side chain orientation with different metals offer an opportunity for subtle optimization of binding specificity not available through conventional organic chemistry. Proof of concept came from two examples of MACs, where the receptor-bound conformation has been previously determined by X-ray crystallography of protein complexes [151]. One was designed to mimic the proposed receptor-bound conformation of the RGD motif of the cyclic pentapeptides c[RGDfMeV] [152] that was confirmed by the crystal structure of the complex with the $\alpha_V\beta_3$ integrin receptor [153]. And the other was designed to mimic the α-amylase-bound conformation of a WRY β-turn motif from tendamistat. Both MACs and sugar-based compounds resemble conventional peptide analogs in that they retain critical amino acid side chains, but differ in that they are devoid of both the peptide backbone and amide surrogates (Figure 11). Turns, owing to the nonrepetitive nature, are structurally diverse motifs and play a special role in mediating protein–protein recognition. They often use the structural-

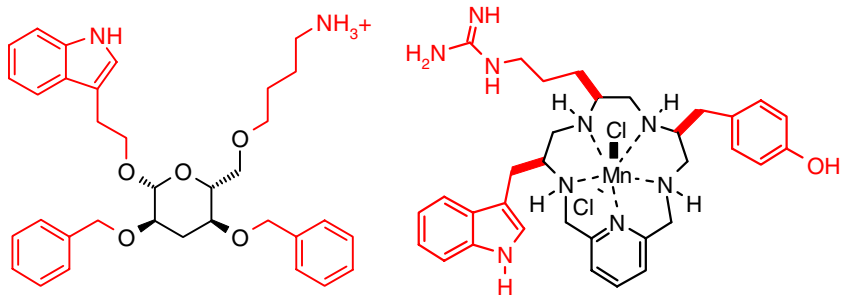

Figure 11. Examples of nonpeptidyl β-turn mimetics, (left) a β-D-glucose based somatostatin inhibitor and (right) a metal complexed of pentaazacrown based amylase inhibitor.

variation strategy to accomplish binding specificities among many receptor subtypes. For example, specific cellular adhesion and migration of cells are recurring themes in embryonic development, tumor metastasis, and wound healing. Many adhesive proteins presented in extracellular matrices contain the common tripeptide sequence, RGD, as their cell-recognition sites. Adhesive recognition involves a number of cell-surface receptors, and each subtype only recognizes the RGD motif in a certain conformation. Both sugar- and MAC-scaffolds provide an excellent platform to tailor molecular diversity. Ideally, this broad structural diversity space should be explored systematically in a scanning-like fashion. The availability of other rigid conformational templates that are synthetically accessible for chiral side chain placement to tailor structural diversity would be extremely useful.

CTP scaffolds

One method is to introduce a covalent linker between residues i and $i+3$, such as head-to-tail cyclization, while retaining the reverse turn conformation. Many natural peptides, with different kinds of biological activities, such as hormones, antibiotics, ion-transport regulators and toxins, are cyclic peptides. They have been reported to bind multiple, unrelated classes of receptors with high affinity. Cyclic peptides are thus considered to be privileged structures capable of providing useful ligands for more than one receptor, presumably due to high content of reverse-turn motifs. For example, cyclic tetrapeptides (CTPs), the minimalist reverse-turn mimetic, have been characterized as potent and highly selective molecules in diverse range of biological areas. In comparison to linear peptides, cyclic peptides are more stable to peptidases, more bioavailable, and possess potential entropic advantages in molecular recognition.

Another method is to incorporate heterochiral dipeptides as residues $i+1$ and $i+2$. Nearly all biological polymers are homochiral. All amino acids in proteins are left-handed, while all sugars in DNA and RNA, and in the metabolic pathways, are right-handed. It is the homochirality of naturally occurring amino acids that allows proteins to adopt regular conformations such as the α-helix and the β-sheet. The incorporation of heterochiral (D,L-alternating) dipeptides into a peptide chain will abruptly change the direction of the peptide (Figure 12). Marshall and his co-workers [154, 155] described theoretical calculations that suggest D-Pro-L-Pro, L-Pro-D-Pro, L-Pro-D-Pip, D-Pro-L-

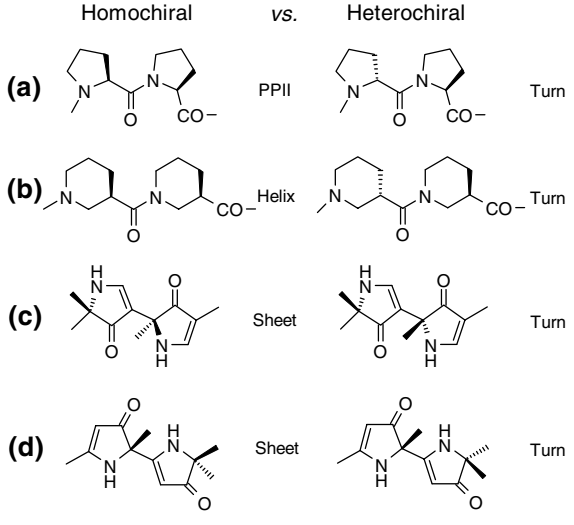

Figure 12. Homochiral dipeptides and dipeptide mimetics usually stabilize regular conformations such as helix and sheet, while heterochiral dipeptides and dipeptide mimetics abruptly change the direction of the peptide.

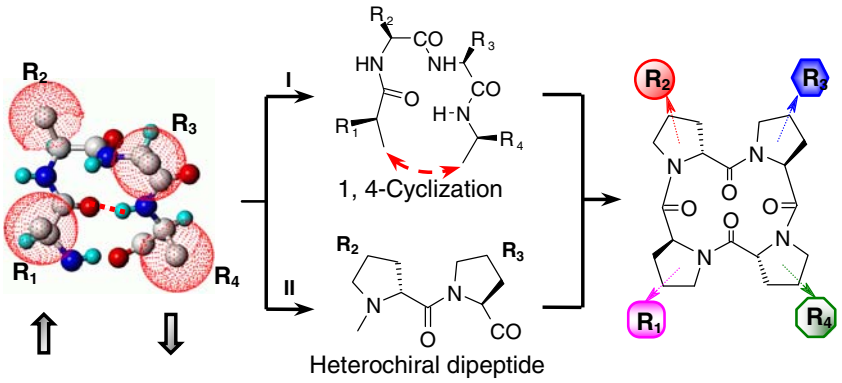

Figure 13. CTP-scaffolds based on heterochiral dipeptides of chimeric amino acids.

Pip, D-Pro-NMe-AA and L-Pro-D-NMe-AA (AA, amino acid other than Gly; Pip, pipecolic amino acid) offer relatively rigid scaffolds on which to orient side chains for interaction with receptors which recognize reverse-turn structures. Gellman and his colleagues [156, 157] suggested that heterochiral dinipecotic acid segments, *R*-Nip-*S*-Nip and *S*-Nip-*R*-Nip, could also promote reverse-turn formation. Smith et al. also established the 3,5- [158, 159] (nitrogen displaced) and 2,5-linked [160] (carbonyl displaced) homochiral polypyrrolinone motif as excellent β-sheet/β-strand mimetics both in the solid state and in solution, and further demonstrated that 3,5-linked heterochiral polypyrrolinones preferentially adopt a turn conformation [161].

Che and Marshall [162] suggested a combined approach – CTPs based on heterochiral dipeptides of chimeric amino acids – to be used as novel conformational templates (Figure 13), for instance, *cyclo*-(D-Pro-L-Pro-D-Pro), as synthetic routes to chimeric prolines containing 2-, 3-, 4-, or 5-substituents are abundant. From our point of view, CTP-scaffolds are excellent candidates for conformational templates because they possess both the required limited conformational flexibility of their peptide backbone and a great diversity of rigidified spatial combination of side chains. First, they are relatively rigid owing to the small 12-membered ring and multiple exocyclic constraints such as the proline rings. Second, derivatives can be prepared readily by solid-phase synthesis [163] or by a convergent solution route [164] with a yield of 85% during the final cyclization in some cases. Third, the presence of four potentially functionalized and stereochemical-controlled centers (α, β, γ and δ carbons) on each proline ring offers seven sites for side chain replacement, providing an overwhelming diversity to custom design molecules. Considering only single substitutions on each proline ring in *cyclo*-(D-Pro-L-Pro-D-Pro), $7^4 = 2401$ unique compounds are possible, all with similar molecular properties due to the same molecular weight and same types of functional groups, but with different orientations of the substituents. This gives the chemists opportunity to custom design molecules to fit a pharmacophoric model and leads to rapid identification of geometrical requirements from compounds active in library screening. In addition to prolines, similar constrained amino acids, including azaproline, pipecolic, azapipecolic, nipecotic, isonipecotic acids and etc., can further tailor structural diversity. An additional advantage of CTP-scaffolds is their stability to proteolytic cleavage due to their cyclic constraint and exocyclic rings, since most proteolytic enzymes do not cleave adjacent to proline residues and/or require access to linear segments of the peptide backbone.

How structurally diverse are these CTP-scaffolds and how do they compare with other scaffolds, such as proteins, sugar- or MAC-based scaffolds? To quantify structural diversity of reverse-turn motifs, the spatial relationships (distances, angles, and virtual torsion angles) of C_α–C_β vectors of approximately 100,000 tetrapeptide structures (regardless of conformations) extracted from a set of high resolution, non-redundant crystal structures of proteins, were subjected to principal component analysis (PCA). Most of the variation in the tetrapeptide structures (70.5%) was explained by the first two components. The following three components with eigenvalues slightly less than

one, together span 21.7% of the overall variance. The first component (PCA1) is highly correlated with the distance between C_{α}^{i} and C_{α}^{i+4}. Instead, the second component (PCA2) is more correlated with the distances between adjacent α carbons. The PCA model suggests that the first component describes the compactness of tetrapeptide motifs, as the α-helices (the most compact secondary structure) clustered to the left with smaller scoring values of PCA1, the β-sheets (the most extended secondary structure) clustered to the right, and reverse turns scattered in the middle. On the other hand, the second component describes the local geometry of tetrapeptide motifs, such as *cis*- or *trans*-amide bonds. The PCA analysis also revealed another noticeable observation. Unlike the regular structural motifs, α-helices or β-sheets, which can be grouped into single clusters, reverse turns are distributed among several distinct sets owing to the non-repetitive nature in backbone torsion values, which results in several subtypes. It also suggests that reverse turns can be classified based solely on side chain orientations, which is more useful for the development and application of reverse turn mimetics, rather than traditional backbone torsion angles. This is the specific aim of one recent study by Tran et al. [165]. A similar analysis was carried out on CTP-scaffolds, with different patterns of substitutions as new sets of virtual C_{α}–C_{β} vectors besides those existing C–C or C–N bonds on the proline rings. The PCA analysis offers an easy way to visualize the structural diversity and to compare CTP-scaffolds with protein structural epitopes (Figure 14). The comparison indicated that most reverse turn conformations can be mimicked effectively with a subset of substitution patterns on the scaffold. In addition, CTP-scaffolds also cover partially the diversity space of α-helices, but overlap little with those of β-sheets. The enormous substitution patterns of CTP-scaffolds are evenly distributed in the structural diversity space, which is particularly useful to custom design molecules for specific side chain orientations. Examples, for mimicking the most common β-turns, type I and II, and their mirror images (of the backbone, but not the side chains), type I′ and II″, are also illustrated in Figure 15. For example, a type-I turn sequence, NKDK, can be mimicked

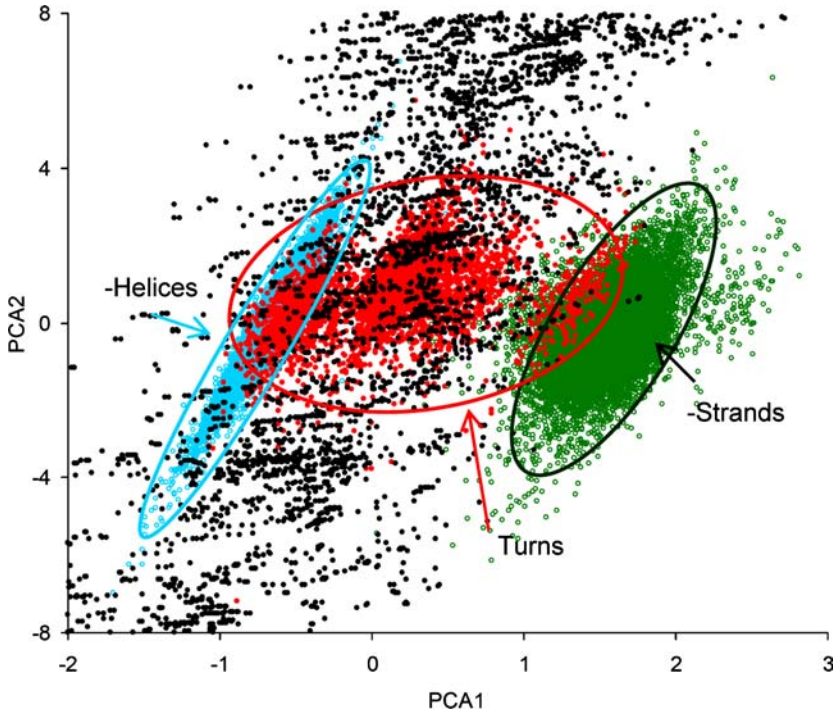

Figure 14. The structural diversity accessible through protein surfaces or CTP-scaffolds. Each point represents a set of four sequential C_{α}–C_{β} vectors in peptides or those vectors derived from appending substituents to a scaffold (α-helix in light blue, β-strand in dark green, turns in red, and CTP-scaffold in black; irregular motifs were omitted for the clarity purpose only).

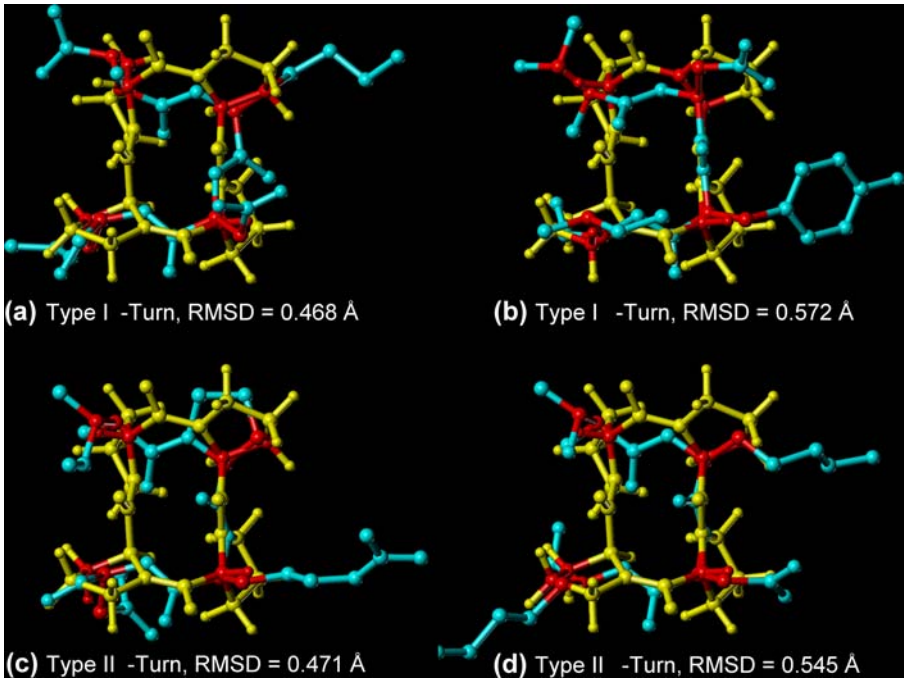

Figure 15. The structure of *cyclo*-(D-Pro-L-Pro-D-Pro-L-Pro) aligned with different types of β-turn motifs: (a) type-I turn (Asn-Lys-Asp-Lys, PDB: 1regX(27–30)), (b) type-I′ turn (Thr-Asp-Tyr-Ile, 1g13A(69–72)), (c) type-II turn (Ile-Pro-Arg-Asn, 1ogoX(61–64)), and (d) type-II′ turn (Thr-Lys-Asp-Lys, 1rypA(229–232)). The CTP scaffolds colored in yellow, the β-turn motifs colored in cyan, and the aligned side chain vectors colored in red, respectively.

with substitutions at the prolines 3-, 3-, 2-, 3-positions, respectively. The RMSD between the C_α–C_β vectors in the type-I turn and the substitution vectors (C_α–C_β, C_α–C_β, C_α–H, and C_β–H, respectively) in the scaffold is 0.468 Å. Very importantly, such substitution pattern not only preorganizes all four χ_1 values, the torsion angle associated with the C_α–C_β bonds, but also fixes orientations of two C_γ–C_δ bonds. These preorganized compounds are particularly useful for determination of the precise spatial requirements for molecular recognition. The opportunity to create molecular diversity in a modular, systematic and tailored way (structurally and functionally) is unique to CTPs, as well as carbohydrates and MACs.

Protein surface recognition and peptidomimetics

Native proteins/peptides can be directly applied as pharmacologically active compounds only to a very limited extent. The major disadvantages of the applications of a peptide in a biological system – for example, rapid degradation by proteases, hepatic clearance, undesired side effects by interaction of conformationally flexible peptides with different receptors, and low membrane permeability – are in most cases detrimental to oral applications. This has led to the concept of peptidomimetics, compounds which have different chemical structures, but still maintain the ability to interact with a specific protein receptor. In other words, a compound which abandons the peptide backbone, but retains those essential chemical functionalities and ability to display them in a characteristic three-dimensional pattern which is complimentary to the protein receptor. For modulating protein interactions, general approaches for mimicking protein surfaces with small molecules would represent a significant advance. The use of conformationally restricted compounds, however, is a ''double-edged sword''. The more one rigidifies a ligand, the less likely it will orient the functionality responsible for complementary interaction with the receptor. While it remains non-trivial to convert a protein surface into a small drug-like molecule with retention of

specific biological activity, a variety of conformational templates imitating different protein secondary structures would be extremely useful as a prelude to develop novel compounds as cellular probes and therapeutic agents such as drugs.

Acknowledgement

This research was supported in part by the Intramural Research Program of the NIH, NHLBI (BRB) and an NIH research grant (GM 68460) to GRM. Y.C. also acknowledges graduate support from the Division of Biology and Biomedical Science of Washington University in St Louis and a postdoctoral fellowship from the National Heart, Lung and Blood Institute. This work is taken in part from his Ph.D. thesis in Molecular Biophysics.

References

1. Che, Y. Ph.D. Thesis, Washington University, 2003.
2. Marshall, G.R., Curr. Opin. Struct. Biol., 2 (1992) 904–919.
3. Marshall, G.R., Tetrahedron, 49 (1993) 3547–3558.
4. Marshall, G.R., Biopolymers, 60 (2001) 246–77.
5. Cochran, A.G., Curr. Opin. Chem. Biol., 5 (2001) 654–659.
6. Toogood, P.L., J. Med. Chem., 45 (2002) 1543–1558.
7. Berg, T., Angew. Chem.-Int. Edit., 42 (2003) 2462–2481.
8. Arkin, M.R. and Wells, J.A., Nat. Rev. Drug Discov., 3 (2004) 301–317.
9. Yin, H., Angew. Chem. Int. Ed., 44 (2005) 4130–4163.
10. Pauling, L., Nature, 161 (1948) 707–709.
11. Lo Conte, L., Chothia, C. and Janin, J., J. Mol. Biol., 285 (1999) 2177–2198.
12. Clackson, T. and Wells, J.A., Science, 267 (1995) 383–386.
13. Bogan, A.A. and Thorn, K.S., J. Mol. Biol., 280 (1998) 1–9.
14. DeLano, W.L., Ultsch, M.H., de Vos, A.M. and Wells, J.A., Science, 287 (2000) 1279–1283.
15. Sidhu, S.S., Fairbrother, W.J. and Deshayes, K., Chembiochem., 4 (2003) 14–25.
16. Kuntz, I.D., Chen, K., Sharp, K.A. and Kollman, P.A., Proc. Natl Acad. Sci. USA, 96 (1999) 9997–10002.
17. Brooijmans, N., Sharp, K.A. and Kuntz, I.D., Proteins, 48 (2002) 645–653.
18. Pabo, C.O. and Sauer, R.T., Annu. Rev. Biochem., 53 (1984) 293–321.
19. Draper, D.E., J. Mol. Biol., 293 (1999) 255–270.
20. Muller, C.W., Curr. Opin. Struct. Biol., 11 (2001) 26–32.
21. Dominguez, R., Trends Biochem. Sci., 29 (2004) 572–578.
22. Tyndall, J.D.A., Nall, T. and Fairlie, D.P., Chem. Rev., 105 (2005) 973–999.
23. Miller, M., Schneider, J., Sathyanarayana, B.K., Toth, M.V., Marshall, G.R., Clawson, L., Selk, L., Kent, S.B.H. and Wlodawer, A., Science, 246 (1989) 1149–1152.
24. Nassar, M., Horn, G., Herrmann, C., Scherer, A., McCormick, F. and Wittinghofer, A., Nature, 375 (1995) 554–560.
25. Harrison, S.C., Cell, 86 (1996) 341–343.
26. Nelson, R., Sawaya, M.R., Balbirnie, M., Madsen, A.O., Riekel, C., Grothe, R. and Eisenberg, D., Nature, 435 (2005) 773–778.
27. Ball, L.J., Kuhne, R., Schneider-Mergener, J. and Oschkinat, H., Angew. Chem. Int. Ed., 44 (2005) 2852–2869.
28. Yu, H.T., Chen, J.K., Feng, S.B., Dalgarno, D.C., Brauer, A.W. and Schreiber, S.L., Cell, 76 (1994) 933–945.
29. Chen, H.I. and Sudol, M., Proc. Natl Acad. Sci. USA, 92 (1995) 7819–7823.
30. Reinhard, M., Rudiger, M., Jockusch, B.M. and Walter, U., FEBS Lett., 399 (1996) 103–107.
31. Freund, C., Dotsch, V., Nishizawa, K., Reinherz, E.L. and Wagner, G., Nat. Struct. Biol., 6 (1999) 656–660.
32. Pornillos, O., Alam, S.L., Davis, D.R. and Sundquist, W.I., Nat. Struct. Biol., 9 (2002) 812–817.
33. Mahoney, N.M., Janmey, P.A. and Almo, S.C., Nat. Struct. Biol., 4 (1997) 953–960.
34. Madden, D.R., Gorga, J.C., Strominger, J.L. and Wiley, D.C., Cell, 70 (1992) 1035–1048.
35. Jardetzky, T.S., Brown, J.H., Gorga, J.C., Stern, L.J., Urban, R.G., Strominger, J.L. and Wiley, D.C., Proc. Natl Acad. Sci. USA, 93 (1996) 734–738.
36. Rose, G.D., Gierasch, L.M. and Smith, J.A., Adv. Protein Chem., 37 (1985) 1–109.
37. Stanfield, R.L., Fieser, T.M., Lerner, R.A. and Wilson, I.A., Science, 248 (1990) 712–719.
38. Rini, J.M., Schulzegahmen, U. and Wilson, I.A., Science, 255 (1992) 959–965.
39. Garcia, K.C., Ronco, P.M., Verroust, P.J., Brunger, A.T. and Amzel, L.M., Science, 257 (1992) 502–507.
40. Tyndall, J.D.A., Pfeiffer, B., Abbenante, G. and Fairlie, D.P., Chem. Rev., 105 (2005) 793–826.
41. Evans, B.E., Rittle, K.E., Bock, M.G., Dipardo, R.M., Freidinger, R.M., Whitter, W.L., Lundell, G.F., Veber, D.F., Anderson, P.S., Chang, R.S.L., Lotti, V.J., Cerino, D.J., Chen, T.B., Kling, P.J., Kunkel, K.A., Springer, J.P. and Hirshfield, J., J. Med. Chem., 31 (1988) 2235–2246.
42. Ripka, W.C., Delucca, G.V., Bach, A.C., Pottorf, R.S. and Blaney, J.M., Tetrahedron, 49 (1993) 3593–3608.
43. Patchett, A.A. and Nargund, R.P., In Doherty, A.M. (Ed), Annual Report in Medicinal Chemistry, Vol. 35. Academic Press Inc, 2000, pp. 289–298.
44. Blackburn, B.K., Lee, A., Baier, M., Kohl, B., Olivero, A.G., Matamoros, R., Robarge, K.D. and McDowell, R.S., J. Med. Chem., 40 (1997) 717–729.
45. Shigeri, Y., Ishikawa, M., Ishihara, Y. and Fujimoto, M., Life Sci., 63 (1998) PL151–PL160.
46. Dziadulewicz, E.K., Brown, M.C., Dunstan, A.R., Lee, W., Said, N.B. and Garratt, P.J., Bioorg. Med. Chem. Lett., 9 (1999) 463–468.
47. Haskell-Luevano, C., Rosenquist, A., Souers, A., Khong, K.C., Ellman, J.A. and Cone, R.D., J. Med. Chem., 42 (1999) 4380–4387.
48. Miller, W.H., Alberts, D.P., Bhatnagar, P.K., Bondinell, W.E., Callahan, J.F., Calvo, R.R., Cousins, R.D., Erhard, K.F., Heerding, D.A., Keenan, R.M., Kwon, C., Manley, P.J., Newlander, K.A., Ross, S.T., Samanen, J.M., Uzinskas, I.N., Venslavsky, J.W., Yuan, C.C.K., Haltiwanger, R.C., Gowen, M., Hwang, S.M., James, I.E., Lark, M.W.,

Rieman, D.J., Stroup, G.B., Azzarano, L.M., Salyers, K.L., Smith, B.R., Ward, K.W., Johanson, K.O. and Huffman, W.F., J. Med. Chem., 43 (2000) 22–26.
49. Liu, Q., Berry, D., Nash, P., Pawson, T., McGlade, C.J. and Li, S.S.C., Mol. Cell, 11 (2003) 471–481.
50. Hashimoto, Y., Kohri, K., Kaneko, Y., Morisaki, H., Kato, T., Ikeda, K. and Nakanishi, M., J. Biol. Chem., 273 (1998) 16544–16550.
51. Smythe, M.L., Huston, S.E. and Marshall, G.R., J. Am. Chem. Soc., 115 (1993) 11594–11595.
52. Marshall, G.R., Head, R.D., Ragno, R., In Di Cera, E., (Ed.), Thermodynamics in Biology, Oxford University Press, Oxford, 2000, pp. 87–111.
53. Marshall, G.R. and Bosshard, H.E., Circ.Res., 31 (1972) 143–150.
54. Marshall, G.R., Hodgkin, E.E., Langs, D.A., Smith, G.D., Zabrocki, J. and Leplawy, M.T., Proc. Natl Acad. Sci. USA, 87 (1990) 487–491.
55. Prasad, B.V.V. and Balaram, P., CRC Crit. Rev. Biochem., 16 (1984) 307–348.
56. Karle, I.L. and Balaram, P., Biochemistry, 29 (1990) 6747–6756.
57. Toniolo, C., Crisma, M., Formaggio, F., Valle, G., Cavicchioni, G., Precigoux, G., Aubry, A. and Kamphuis, J., Biopolymers, 33 (1993) 1061–1072.
58. Garcia-Echeverria, C., Chene, P., Blommers, M.J.J. and Furet, P., J. Med. Chem., 43 (2000) 3205–3208.
59. Marqusee, S. and Baldwin, R.L., Proc. Natl Acad. Sci. USA, 84 (1987) 8898–8902.
60. Albert, J.S. and Hamilton, A.D., Biochemistry, 34 (1995) 984–990.
61. Butterfield, S.M., Patel, P.R. and Waters, M.L., J. Am. Chem. Soc., 124 (2002) 9751–9755.
62. FernandezRecio, J., Vazquez, A., Civera, C., Sevilla, P. and Sancho, J., J. Mol. Biol., 267 (1997) 184–197.
63. Viguera, A.R. and Serrano, L., Biochemistry, 34 (1995) 8771–8779.
64. Jackson, D.Y., King, D.S., Chmielewski, J., Singh, S. and Schultz, P.G., J. Am. Chem. Soc., 113 (1991) 9391–9392.
65. Leduc, A.M., Trent, J.O., Wittliff, J.L., Bramlett, K.S., Briggs, S.L., Chirgadze, N.Y., Wang, Y., Burris, T.P. and Spatola, A.F., Proc. Natl Acad. Sci. USA, 100 (2003) 11273–11278.
66. Felix, A.M., Heimer, E.P., Wang, C.T., Lambros, T.J., Fournier, A., Mowles, T.F., Maines, S., Campbell, R.M., Wegrzynski, B.B., Toome, V., Fry, D. and Madison, V.S., Int. J. Pept. Protein Res., 32 (1988) 441–454.
67. Osapay, G. and Taylor, J.W., J. Am. Chem. Soc., 114 (1992) 6966–6973.
68. Bracken, C., Gulyas, J., Taylor, J.W. and Baum, J., J. Am. Chem. Soc., 116 (1994) 6431–6432.
69. Taylor, J.W., Biopolymers, 66 (2002) 49–75.
70. Shepherd, N.E., Abbenante, G. and Fairlie, D.P., Angew. Chem. Int. Ed., 43 (2004) 2687–2690.
71. Shepherd, N.E., Hoang, H.N., Abbenante, G. and Fairlie, D.P., J. Am. Chem. Soc., 127 (2005) 2974–2983.
72. Schievano, E., Pagano, K., Mammi, S. and Peggion, E., Biopolymers, 80 (2005) 294–302.
73. Blackwell, H.E. and Grubbs, R.H., Angew. Chem. Int. Ed., 37 (1998) 3281–3284.
74. Schafmeister, C.E., Po, J. and Verdine, G.L., J. Am. Chem. Soc., 122 (2000) 5891–5892.
75. Walensky, L.D., Kung, A.L., Escher, I., Malia, T.J., Barbuto, S., Wright, R.D., Wagner, G., Verdine, G.L. and Korsmeyer, S.J., Science, 305 (2004) 1466–1470.
76. Phelan, J.C., Skelton, N.J., Braisted, A.C. and McDowell, R.S., J. Am. Chem. Soc., 119 (1997) 455–460.
77. Fujimoto, K., Oimoto, N., Katsuno, K., Inouye, M., Chem. Commun., (2004) 1280–1281.
78. Ghadiri, M.R. and Choi, C., J. Am. Chem. Soc., 112 (1990) 1630–1632.
79. Ghadiri, M.R. and Fernholz, A.K., J. Am. Chem. Soc., 112 (1990) 9633–9635.
80. Kelso, M.J., Hoang, H.N., Appleton, T.G. and Fairlie, D.P., J. Am. Chem. Soc., 122 (2000) 10488–10489.
81. Kelso, M.J., Hoang, H.N., Oliver, W., Sokolenko, N., March, D.R., Appleton, T.G. and Fairlie, D.P., Angew. Chem. Int. Ed., 42 (2003) 421–424.
82. Kelso, M.J., Beyer, R.L., Hoangt, H.N., Lakdawala, A.S., Snyder, J.P., Oliver, W.V., Robertson, T.A., Appleton, T.G. and Fairlie, D.P., J. Am. Chem. Soc., 126 (2004) 4828–4842.
83. Ruan, F.Q., Chen, Y.Q. and Hopkins, P.B., J. Am. Chem. Soc., 112 (1990) 9403–9404.
84. Gilbertson, S.R. and Wang, X.F., J. Org. Chem., 61 (1996) 434–435.
85. Cabezas, E. and Satterthwait, A.C., J. Am. Chem. Soc., 121 (1999) 3862–3875.
86. Chapman, R.N., Dimartino, G. and Arora, P.S., J. Am. Chem. Soc., 126 (2004) 12252–12253.
87. Calvo, J.C., Choconta, K.C., Diaz, D., Orozco, O., Bravo, M.M., Espejo, F., Salazar, L.M., Guzman, F. and Patarroyo, M.E., J. Med. Chem., 46 (2003) 5389–5394.
88. Kemp, D.S., Boyd, J.G. and Muendel, C.C., Nature, 352 (1991) 451–454.
89. Kemp, D.S., Curran, T.P., Davis, W.M., Boyd, J.G. and Muendel, C., J. Org. Chem., 56 (1991) 6672–6682.
90. Kemp, D.S., Curran, T.P., Boyd, J.G. and Allen, T.J., J. Org. Chem., 56 (1991) 6683–6697.
91. Kemp, D.S., Allen, T.J. and Oslick, S.L., J. Am. Chem. Soc., 117 (1995) 6641–6657.
92. Kemp, D.S., Allen, T.J., Oslick, S.L. and Boyd, J.G., J. Am. Chem. Soc., 118 (1996) 4240–4248.
93. Kemp, D.S., Oslick, S.L. and Allen, T.J., J. Am. Chem. Soc., 118 (1996) 4249–4255.
94. Maison, W., Arce, E., Renold, P., Kennedy, R.J. and Kemp, D.S., J. Am. Chem. Soc., 123 (2001) 10245–10254.
95. Austin, R.E., Maplestone, R.A., Sefler, A.M., Liu, K., Hruzewicz, W.N., Liu, C.W., Cho, H.S., Wemmer, D.E. and Bartlett, P.A., J. Am. Chem. Soc., 119 (1997) 6461–6472.
96. Simon, R.J., Kania, R.S., Zuckermann, R.N., Huebner, V.D., Jewell, D.A., Banville, S., Ng, S., Wang, L., Rosenberg, S., Marlowe, C.K., Spellmeyer, D.C., Tan, R.Y., Frankel, A.D., Santi, D.V., Cohen, F.E. and Bartlett, P.A., Proc. Natl Acad. Sci. USA, 89 (1992) 9367–9371.
97. Armand, P., Kirshenbaum, K., Goldsmith, R.A., Farr-Jones, S., Barron, A.E., Truong, K.T.V., Dill, K.A., Mierke, D.F., Cohen, F.E., Zuckermann, R.N. and Bradley, E.K., Proc. Natl Acad. Sci. USA, 95 (1998) 4309–4314.
98. Gellman, S.H., Acc. Chem. Res., 31 (1998) 173–180.
99. Seebach, D., Kimmerlin, T., Sebesta, R., Campo, M.A. and Beck, A.K., Tetrahedron, 60 (2004) 7455–7506.

100. Hara, T., Durell, S.R., Myers, M.C., Appella, D.H., J. Am. Chem. Soc., 128 (2006) 1995–2004.
101. Hart, S.A., Bahadoor, A.B.F., Matthews, E.E., Qiu, X.Y.J. and Schepartz, A., J. Am. Chem. Soc., 125 (2003) 4022–4023.
102. Kritzer, J.A., Lear, J.D., Hodsdon, M.E. and Schepartz, A., J. Am. Chem. Soc., 126 (2004) 9468–9469.
103. Stephens, O.M., Kim, S., Welch, B.D., Hodsdon, M.E., Kay, M.S. and Schepartz, A., J. Am. Chem. Soc., 127 (2005) 13126–13127.
104. Orner, B.P., Ernst, J.T. and Hamilton, A.D., J. Am. Chem. Soc., 123 (2001) 5382–5383.
105. Ernst, J.T., Kutzki, O., Debnath, A.K., Jiang, S., Lu, H. and Hamilton, A.D., Angew. Chem. Int. Ed., 41 (2002) 278–281.
106. Kutzki, O., Park, H.S., Ernst, J.T., Orner, B.P., Yin, H. and Hamilton, A.D., J. Am. Chem. Soc., 124 (2002) 11838–11839.
107. Yin, H., Lee, G.I., Sedey, K.A., Kutzki, O., Park, H.S., Omer, B.P., Ernst, J.T., Wang, H.G., Sebti, S.M. and Hamilton, A.D., J. Am. Chem. Soc., 127 (2005) 10191–10196.
108. Yin, H., Lee, G.I., Park, H.S., Payne, G.A., Rodriguez, J.M., Sebti, S.M. and Hamilton, A.D., Angew. Chem. Int. Ed., 44 (2005) 2704–2707.
109. Jacoby, E., Bioorg. Med. Chem. Lett., 12 (2002) 891–893.
110. Ernst, J.T., Becerril, J., Park, H.S., Yin, H. and Hamilton, A.D., Angew. Chem. Int. Ed., 42 (2003) 535–539.
111. Davis, J.M., Truong, A. and Hamilton, A.D., Org. Lett., 7 (2005) 5405–5408.
112. Tugarinov, V., Zvi, A., Levy, R. and Anglister, J., Nat. Struct. Biol., 6 (1999) 331–335.
113. Wittelsberger, A., Keller, M., Scarpellino, L., Patiny, L., Acha-Orbea, H. and Mutter, M., Angew. Chem. Int. Ed., 39 (2000) 1111–1115.
114. Freidinger, R.M., Perlow, D.S. and Veber, D.F., J. Org. Chem., 47 (1982) 104–109.
115. Nagai, U., Sato, K., Nakamura, R. and Kato, R., Tetrahedron, 49 (1993) 3577–3592.
116. Cluzeau, J. and Lubell, W.D., Biopolymers, 80 (2005) 98–150.
117. Hinds M.G., Richards N.G.J., Robinson J.A., 1988, J. Chem. Soc. Chem. Commun., 1447–1449.
118. Hinds, M.G., Welsh, J.H., Brennand, D.M., Fisher, J., Glennie, M.J., Richards, N.G.J., Turner, D.L. and Robinson, J.A., J. Med. Chem., 34 (1991) 1777–1789.
119. Ward, P., Ewan, G.B., Jordan, C.C., Ireland, S.J., Hagan, R.M. and Brown, J.R., J. Med. Chem., 33 (1990) 1848–1851.
120. Genin, M.J. and Johnson, R.L., J. Am. Chem. Soc., 114 (1992) 8778–8783.
121. Zerkout, S., Dupont, V., Aubry, A., Vidal, J., Collet, A., Vicherat, A. and Marraud, M., Int. J. Pept. Protein Res., 44 (1994) 378–387.
122. Bach, A.C. and Gierasch, L.M., J. Am. Chem. Soc., 107 (1985) 3349–3350.
123. Bach, A.C. and Gierasch, L.M., Biopolymers, 25 (1986) S175–S191.
124. Chauhan, V.S., Sharma, A.K., Uma, K., Paul, P.K.C. and Balaram, P., Int. J. Pept. Protein Res., 29 (1987) 126–133.
125. Palmer, D.E., Pattaroni, C., Nunami, K., Chadha, R.K., Goodman, M., Wakamiya, T., Fukase, K., Horimoto, S., Kitazawa, M., Fujita, H., Kubo, A. and Shiba, T., J. Am. Chem. Soc., 114 (1992) 5634–5642.
126. Tian, Z.Q. and Bartlett, P.A., J. Am. Chem. Soc., 118 (1996) 943–949.
127. Marshall, G.R., Humblet, C., Opdenbosch, V., Zabrocki, J., In Rich, D.H. and Gross, E., (Ed.), Peptides: Synthesis-Structure-Function. Proceedings of the 7th American Peptide Symposium, Pierce Chemical Co., Rockford, IL, 1981, pp. 669–672.
128. Zabrocki, J., Smith, G.D., Dunbar, J.B., Iijima, H. and Marshall, G.R., J. Am. Chem. Soc., 110 (1988) 5875–5880.
129. Smith, G.D., Zabrocki, J., Flak, T.A. and Marshall, G.R., Int. J. Pept. Protein Res., 37 (1991) 191–197.
130. Zabrocki, J., Dunbar, J.B., Marshall, K.W., Toth, M.V. and Marshall, G.R., J. Org. Chem., 57 (1992) 202–209.
131. Nachman, R.J., Zabrocki, J., Olczak, J., Williams, H.J., Moyna, G., Scott, A.I. and Coast, G.M., Peptides, 23 (2002) 709–716.
132. Hitotsuyanagi, Y., Motegi, S., Fukaya, H. and Takeya, K., J. Org. Chem., 67 (2002) 3266–3271.
133. Sukumaran, D.K., Prorok, M. and Lawrence, D.S., J. Am. Chem. Soc., 113 (1991) 706–707.
134. Brady, S.F., Paleveda, W.J., Arison, B.H., Saperstein, R., Brady, E.J., Raynor, K., Reisine, T., Veber, D.F. and Freidinger, R.M., Tetrahedron, 49 (1993) 3449–3466.
135. Curran, T.P. and McEnaney, P.M., Tetrahedron Lett., 36 (1995) 191–194.
136. Tong, Y.S., Olczak, J., Zabrocki, J., Gershengorn, M.C., Marshall, G.R. and Moeller, K.D., Tetrahedron, 56 (2000) 9791–9800.
137. Hoffmann, T., Lanig, H., Waibel, R. and Gmeiner, P., Angew. Chem. Int. Ed., 40 (2001) 3361–3364.
138. Muller, G., Gurrath, M., Kurz, M. and Kessler, H., Proteins, 15 (1993) 235–251.
139. Che, Y., Marshall, G.R., Biopolymers, 81 (2006) 392–406.
140. Magaard, V.W., Sanchez, R.M., Bean, J.W. and Moore, M.L., Tetrahedron Lett., 34 (1993) 381–384.
141. Beausoleil, E. and Lubell, W.D., J. Am. Chem. Soc., 118 (1996) 12902–12908.
142. Keller, M., Sager, C., Dumy, P., Schutkowski, M., Fischer, G.S. and Mutter, M., J. Am. Chem. Soc., 120 (1998) 2714–2720.
143. Lecoq, A., Boussard, G., Marraud, M. and Aubry, A., Biopolymers, 33 (1993) 1051–1059.
144. Zhang, W.J., Berglund, A., Kao, J.L.F., Couty, J.P., Gershengom, M.C. and Marshall, G.R., J. Am. Chem. Soc., 125 (2003) 1221–1235.
145. Che, Y. and Marshall, G.R., J. Org. Chem., 69 (2004) 9030–9042.
146. Hartley, O., Gaertner, H., Wilken, J., Thompson, D., Fish, R., Ramos, A., Pastore, C., Dufour, B., Cerini, F., Melotti, A., Heveker, N., Picard, L., Alizon, M., Mosier, D., Kent, S. and Offord, R., Proc. Natl Acad. Sci. USA, 101 (2004) 16460–16465.
147. Hirschmann, R., Nicolaou, K.C., Pietranico, S., Salvino, J., Leahy, E.M., Sprengeler, P.A., Furst, G., Smith, A.B., Strader, C.D., Cascieri, M.A., Candelore, M.R., Donaldson, C., Vale, W. and Maechler, L., J. Am. Chem. Soc., 114 (1992) 9217–9218.
148. Hirschmann, R., Nicolaou, K.C., Pietranico, S., Leahy, E.M., Salvino, J., Arison, B., Cichy, M.A., Spoors, P.G., Shakespeare, W.C., Sprengeler, P.A., Hamley, P., Smith, A.B., Reisine, T., Raynor, K., Maechler, L., Donaldson, C., Vale, W., Freidinger, R.M., Cascieri, M.R. and Strader, C.D., J. Am. Chem. Soc., 115 (1993) 12550–12568.

149. Hirschmann, R., Hynes, J., Cichy-Knight, M.A., van Rijn, R.D., Sprengeler, P.A., Spoors, P.G., Shakespeare, W.C., Pietranico-Cole, S., Barbosa, J., Liu, J., Yao, W.Q., Rohrer, S. and Smith, A.B., J. Med. Chem., 41 (1998) 1382–1391.
150. Reaka, A.J., Ho, C.M. and Marshall, G.R., J. Comput. Aided Mol. Des., 16 (2002) 585–600.
151. Zhang, W.-J., Wu, Y., Gao, Y., Poreddy, A.R., Slomczynska, U., Chang, L., Weber, M.E., Marshall, G.R., In Chorev, M. and Sawyer, T.K., (Eds.), Peptide Revolution: Genomics, Proteomics and Therapeutics: Proceedings of the 18th American Peptide Symposium, Boston, MA, 2003, pp. 196–197.
152. Nikiforovich, G.V., Kover, K.E., Zhang, W.J. and Marshall, G.R., J. Am. Chem. Soc., 122 (2000) 3262–3273.
153. Xiong, J.P., Stehle, T., Zhang, R.G., Joachimiak, A., Frech, M., Goodman, S.L. and Aranout, M.A., Science, 296 (2002) 151–155.
154. Chalmers, D.K. and Marshall, G.R., J. Am. Chem. Soc., 117 (1995) 5927–5937.
155. Takeuchi, Y. and Marshall, G.R., J. Am. Chem. Soc., 120 (1998) 5363–5372.
156. Chung, Y.J., Christianson, L.A., Stanger, H.E., Powell, D.R. and Gellman, S.H., J. Am. Chem. Soc., 120 (1998) 10555–10556.
157. Chung, Y.J., Huck, B.R., Christianson, L.A., Stanger, H.E., Krauthauser, S., Powell, D.R. and Gellman, S.H., J. Am. Chem. Soc., 122 (2000) 3995–4004.
158. Smith, A.B., Keenan, T.P., Holcomb, R.C., Sprengeler, P.A., Guzman, M.C., Wood, J.L., Carroll, P.J. and Hirschmann, R., J. Am. Chem. Soc., 114 (1992) 10672–10674.
159. Smith, A.B., Guzman, M.C., Sprengeler, P.A., Keenan, T.P., Holcomb, R.C., Wood, J.L., Carroll, P.J. and Hirschmann, R., J. Am. Chem. Soc., 116 (1994) 9947–9962.
160. Smith, A.B., Knight, S.D., Sprengeler, P.A. and Hirschmann, R., Bioorg. Med. Chem., 4 (1996) 1021–1034.
161. Smith, A.B., Wang, W.Y., Sprengeler, P.A. and Hirschmann, R., J. Am. Chem. Soc., 122 (2000) 11037–11038.
162. Che, Y. and Marshall, G.R., J. Med. Chem., 49 (2006) 111–124.
163. Mastle, W., Weber, T., Thewalt, U. and Rothe, M., Biopolymers, 28 (1989) 161–174.
164. Gilbertson, S.R. and Pawlick, R.V., Tetrahedron Lett., 36 (1995) 1229–1232.
165. Tran, T.T., McKie, J., Meutermans, W.D.F., Bourne, G.T., Andrews, P.R., Smythe, M.L., J. Comput. Aided Mol. Des., 19 (2005) 551–566.